European Review for Medical and Pharmacological Sciences 2020; 24: 1007-1022

LINC00662 triggers malignant progression of chordoma by the activation of RNF144B *via* targeting miR-16-5p

C.-B. WANG[1], Y. WANG[2], J.-J. WANG[1], X.-L. GUO[3]

[1]Department of Orthopedics, Yantaishan Hospital, Yantai, Shandong, China
[2]Health Care Center, Lize Street Community, Economic and Technological Development District, China
[3]Department of Neurology, Yantaishan Hospital, Yantai, Shandong, China

Abstract. – OBJECTIVE: Chordoma is a rare malignant tumor difficult to diagnose and treat. Long non-coding RNAs acting as novel biomarkers are frequently reported in numerous cancers. The purpose of this study was to investigate the role of long intergenic non-coding RNA 00662 (LINC00662) and its associated action mechanisms in chordoma.

MATERIALS AND METHODS: The expression of LINC00662, Ring finger protein 144B (RNF144B), and microRNA-16-5p (miR-16-5p) was detected by quantitative Real Time-Polymerase Chain Reaction (qRT-PCR). The protein levels of RNF144B, cell proliferation markers (Cyclin D1 and Ki67), epithelial-mesenchymal transition (EMT) markers (E-cadherin, Vimentin and N-cadherin), and glycolysis markers [glucose transporter 1 (GLUT1), hexokinase II (HK2), and lactic dehydrogenase A (LDHA)] were determined by Western blot. Cell proliferation, the number of colonies, migration, and invasion were investigated by 3-(4, 5-dimethyl-2-thiazolyl)-2, 5-diphenyl-2-H-tetrazolium bromide (MTT), colony formation, and transwell assays, respectively. Glycolysis progress was evaluated by the glycolysis stress test, glucose consumption, lactate production, and ATP production. The relationship between miR-16-5p and LINC00662 or RNF144B was predicted by the online bioinformatics tool starBase and verified by Dual-Luciferase reporter assay. Xenograft tumor model was established to monitor the role of LINC00662 *in vivo*.

RESULTS: LINC00662 and RNF144B were aberrantly upregulated in chordoma tissues. Knockdown of LINC00662 or RNF144B impeded proliferation, colony formation, invasion, migration, EMT, and glycolysis in chordoma cells. Besides, RNF144B overexpression reversed the role of LINC00662 knockdown. It was confirmed that miR-16-5p was a target of LINC00662, and miR-16-5p could target RNF144B. The relationship between LINC00662 and RNF144B was established by miR-16-5p. In addition, LINC00662 stable knockdown inhibited tumor growth *in vivo*.

CONCLUSIONS: LINC00662 participated in the malignant progression of chordoma by the promotion of RNF144B by acting as a sponge of miR-16-5p, suggesting that LINC00662 was a promising therapeutic target for chordoma.

Key Words:
LINC00662, RNF144B, MiR-16-5p, Chordoma

Introduction

Chordoma, an uncommon malignant tumor, originates from the primary malignant bone tumor of the original spinal cord tissues[1]. Primary tumors occur along the spine, with around 1/3 of the cases developing in the clivus, mobile spine, and sacrum[2]. Chordoma has strong local invasiveness and a high recurrence rate[3]. According to statistics, the 5-year and 10-year survival rates of patients with chordoma are about 68% and 40%, respectively[2]. Despite the most advanced skull base surgery techniques, chordoma is difficult to eradicate by surgery because critical anatomical locations and tumor volumes rarely allow extensive radical resection[4,5]. Besides, chordoma grows with occult, non-specific symptoms[6,7]. Therefore, there is an urgent need to identify novel biomarkers to improve the diagnosis and treatment of chordoma.

Long non-coding RNAs (lncRNAs) are a cluster of non-coding RNA molecules longer than 200 nucleotides[8]. The expression of lncRNAs is specific in diverse cell types, tissues at indicated developmental stages, as well as in different diseases, including cancer[9,10], and the crucial role of lncRNAs in cancers has aroused much attention. Unfortunately, there is a lack of attention and research on the function of lncRNAs in chordoma mainly due to the rarity of chordoma. However, the specific regulatory effects of lncRNAs in chordoma cannot be underestimated.

Corresponding Author: Xiuli Guo, MM; e-mail: kjmxkw@163.com

A previous study elucidated that the low expression of lncRNA LOC554202 was linked to the inhibitory proliferation, migration, and invasion of chordoma cells[11], indicating the vital role of lncRNA during the development of chordoma. Long intergenic non-coding RNAs (lincRNAs) are one of the types of lncRNAs and share similar characteristics with other transcripts of lncRNAs family, making up over half of lncRNAs transcripts[12,13]. LincRNA 00662 (LINC00662), one of the lincRNAs, was mentioned to be involved in a host of cancers. However, the role of LINC00662 in chordoma was not mentioned yet. It was worth exploring whether LINC00662 functioned in chordoma.

MicroRNAs (miRNAs) are also a class of non-coding RNAs with short length containing ~23 nucleotides[14]. MiRNAs inhibit gene expression at post-transcriptional and translational levels *via* interacting with certain binding sites in 3' untranslated region (3' UTR) of targeted messenger RNAs (mRNAs)[15]. The dysregulation of miRNAs in human cancers participated in the progression of cancer[16], including miR-16-5p. The involvement of miR-16-5p was reported in dozens of cancers, such as breast cancer, lung cancer, and mesothelioma[17-19]. Consistently, miR-16-5p functioned in these cancers by acting as a tumor suppressor. Interestingly, Zhang et al[20] partially clarified the role of miR-16-5p in chordoma. However, the diverse action mode and mechanism of miR-16-5p in chordoma still need to be explored.

Ring finger protein 144B (RNF144B), also known as PIR2, is an E3-ubiquitin ligase that is substantial for the participation in cancers[21,22]. Unfortunately, the research of the RNF144B function in chordoma was insufficient and lacking. Only Ma et al[11] asserted that RNF144B was an oncogene to regulate cell proliferation and invasion in chordoma, indicating the vital role of RNF144B in chordoma. Hence, more information about the functional role of RNF144B and associated action mechanism should be investigated in chordoma.

In our research, we examined the expression of LINC00662 and RNF144B in chordoma tissues. The gain-function or loss-function experiments were performed to determine their potential functions in chordoma cells. Besides, a novel action mechanism of LINC00662 was also elucidated. The aim of this study was to further understand the mechanism of chordoma development and provide novel biomarkers to identify and treat chordoma.

Materials and Methods

Tissues

The chordoma tissues (n=30) and adjacent non-tumor tissues (n=30) were collected from chordoma patients in the Yantaishan Hospital. These tissues were frozen in liquid nitrogen after excision and then stored in -80°C storage. The informed consent was obtained from each patient. This research was approved by the Ethics Committee of the Yantaishan Hospital.

Quantitative Real Time-Polymerase Chain Reaction (qRT-PCR)

Rneasy MiNi Kit (Qiagen, Hilden, Germany) was utilized to extract total RNA from chordoma tissues and cells. After the measurement of concentration and integrity of total RNA, reverse transcription was executed using RT2 First Strand Kit (Qiagen, Hilden, Germany) or miScript II RT Kit (Qiagen, Hilden, Germany). Afterwards, RT2 SYBR Green FAST Mastermix (Qiagen, Hilden, Germany) or miScript SYBR Green PCR Kit (Qiagen, Hilden, Germany) were used for amplification reaction under a Real Time-PCR system (Applied Biosystems, Foster City, CA, USA). The relative expression was normalized by β-actin or U6 and calculated using the $2^{-\Delta\Delta Ct}$ method. The primers used were listed as below: LINC00662: 5'-ACTAACAAGCTGGGTGCAGA-3' (forward) and 5'-CCTCCTGGTCTGCGAGAAAT-3' (reverse); RNF144B: 5'-ATGGGCTCAGCTGGTAGGC-3' (forward) and 5'-GGTTGTGGATGGGTCGTGCT-3' (reverse); miR-16-5p: 5'-TAGCAGCACGTAAATATTGGCG-3' (forward) and 5'-TGCGTGTCGTGGAGTC-3' (reverse); U6**:** 5'-GCUUCGGCAGCACAUAUACUAAAAU-3' (forward) and 5'-CGCUUCACGAAUUUGCGUGUCAU-3' (reverse) and β-actin**:** 5'-GATATTGCTGCGCTCGTTG-3' (forward) and 5'-TTCAGGGTCAGGATACCTCTTT-3' (reverse).

Western Blot

Western blot was executed according to the previous methods[23]. In brief, the proteins were transferred onto polyvinylidene difluoride (PVDF) membranes (Bio-Rad, Hercules, CA, USA) after the separation. Next, the membrane was placed in blocking solution containing 5% skim milk and probed with the primary antibodies against RNF144B (PA5-39152; 1:1000; Invitrogen, Carlsbad, CA, USA), Cyclin D1 (MA5-16356; 1:200; Invitrogen, Carlsbad, CA, USA),

Ki67 (ab16667; 1:1000; Abcam, Cambridge, MA, USA), E-cadherin (ab1416; 1:50; Abcam, Cambridge, MA, USA), Vimentin (ab92547; 1:1000; Abcam, Cambridge, MA, USA), N-cadherin (ab18203; 1:1000; Abcam, Cambridge, MA, USA), glucose transporter 1 (GLUT1) (ab115730; 1:100000; Abcam, Cambridge, MA, USA), hexokinase II (HK2) (ab104836; 1:1000; Abcam, Cambridge, MA, USA), lactic dehydrogenase A (LDHA) (ab135366; 1:1000; Abcam, Cambridge, MA, USA), and β-actin (ab6276; 1:5000; Abcam, Cambridge, MA, USA) and the secondary antibodies (ab205718 and ab205719; 1:5000; Abcam, Cambridge, MA, USA). Finally, the protein blots on the membranes were appeared using an enhanced chemiluminescence (ECL) kit (Beyotime, Shanghai, China).

Cell Lines

Chordoma cell lines (U-CH1 and U-CH2) were obtained from American Type Culture Collection (ATCC; Manassas, VA, USA). Roswell Park Memorial Institute-1640 medium (RPMI-1640; Life Technologies, Carlsbad, CA, USA) supplemented with 10% fetal bovine serum (FBS; Life Technologies) was used to culture these cells in a humidified condition with 5% CO_2 at 37°C.

Cell Transfection

Small interference RNA (siRNA) against LINC00662 and RNF144B (si-LINC00662 and si-RNF144B) and their negative control (si-NC) were synthesized by Sangon Biotechnology (Shanghai, China). RNF144B sequence fragment was constructed onto the pcDNA3.1 vector, named as pcDNA-RNF144B, which was accomplished by Sangon Biotechnology, pcDNA3.1 empty vector (pcDNA) as the control. MiR-16-5p mimics (miR-219-5p), miR-16-5p inhibitor (anti-miR-16-5p), and their corresponding negative controls (miR-NC and anti-NC) were purchased from Ribobio (Guangzhou, China). Lentiviral vector (lenti-short hairpin sh-LINC00662) and its negative control (sh-NC) were assembled by Genechem (Shanghai, China). The U-CH1 and U-CH2 cells were subjected to transfection using Lipofectamine 3000 (Invitrogen, Carlsbad, CA, USA). The following experiments were conducted at 48 h post-transfection.

3-(4,5-dimethyl-2-thiazolyl)-2,5-diphenyl-2-H-tetrazolium bromide (MTT) assay

U-CH1 and U-CH2 cells with different transfection were seeded into 96-well plates (5×10^3 cells/well) (Corning Costar, Corning, NY, USA). After the treatment of 10 μL MTT solution (Beyotime, Shanghai, China) at the indicated time points (0 h, 24 h, 48 h and 72 h) for 4 h at 37°C, the dimethyl sulfoxide (DMSO; Beyotime, Shanghai, China) was pipetted into each well to dissolve the formazan. The absorbance at 490 nm was checked using the Multiskan Ascent (Thermo Fisher Scientific, Waltham, MA, USA) to assess cell proliferation.

Colony Formation Assay

U-CH1 and U-CH2 cells with different transfection were digested with trypsin and seeded into 6-well plates (5×10^3 cells/well) (Corning Costar, Corning, NY, USA) for 2 weeks. Subsequently, the colonies derived from U-CH1 and U-CH2 cells were fixed with methanol and stained with 0.1% crystal violet for 20 minutes. Next, the number of colonies was investigated *via* a microscope (Olympus, Tokyo, Japan) and Image J software.

Transwell Assay

U-CH1 and U-CH2 cells (1×10^5 cells/mL) were resuspended in fresh RPMI-1640 medium containing 10% FBS. Then, the suspensions were pipetted into the top of 6-well transwell chambers (Corning Costar, Corning, NY, USA), and RPMI-1640 medium containing 10% FBS was added into the bottom of the chambers. After culturing for 24 h, the migrated cells in the lower surface were fixed with methanol and stained with 0.1% crystal violet. The cells in five random fields were counted using a microscope (Olympus, Tokyo, Japan). Noteworthily, cell invasion was also conducted using the same method, except that the upper transwell chambers needed to be pre-coated with Matrigel (Corning Costar, Corning, NY, USA).

Glycolysis Stress Test

U-CH1 and U-CH2 cells were seeded into RPMI-1640 medium without glucose or pyruvate and incubated for at least 30 min before the assay in a 37°C incubator without CO_2; then, the baseline extracellular acidification rate (ECAR, a pointer of glycolytic lactate production) was measured using the XF96 Analyzer (Seahorse Bioscience, Billerica, MA, USA). Glucose (10 mM; Sigma-Aldrich, St. Louis, MO, USA) was provided to detect the glycolysis rate according to the rapidly increased ECAR value. Next, the addition of oligomycin (5 μM; Sigma-Aldrich, St. Louis, MO, USA) was used to inhibit mitochondrial ATP production and transform the energy production

to glycolysis, with the increase of ECAR reflecting the maximum glycolytic capacity. The final addition was 2-deoxyglucose (2-DG, Sigma-Aldrich, St. Louis, MO, USA), which was used to suppress glycolysis by specifically binding to hexokinase, leading to a decline of ECAR rate, which confirmed that the ECAR production was due to glycolysis. The glycolytic reserve is the difference between glycolytic capacity and glycolysis rate, which represented the capability of the cells to respond to energetic requirements.

Glucose Consumption, Lactate Production and ATP Production Assay

The glycolysis progression was evaluated according to glucose consumption, lactate production, and ATP production using Glucose Assay Kit (Biovision, Milpitas, CA, USA), Lactate Assay Kit (Biovision, Milpitas, CA, USA), and ATP Assay Kit (Beyotime) in line with the product's instruction, respectively.

Bioinformatics Analysis

The Online bioinformatics database starBase (http://starbase.sysu.edu.cn/) was chosen to predict the potential target genes of lncRNA or miRNA and analyze the corresponding specific binding sites.

Dual-Luciferase Reporter Assay

The wild-type (WT) sequences of LINC00662 (LINC00662-WT) harboring the binding sites with miR-16-5p and matched mutant (MUT) sequences of LINC00662 (LINC00662-MUT) were amplified and constructed onto the pGL4 vector (Promega, Madison, WI, USA), respectively. Likewise, the WT sequences of RNF144B 3' UTR (RNF144B 3' UTR-WT) harboring the binding sites with miR-16-5p and matched MUT sequences harboring the mutated binding sites with miR-16-5p (RNF144B 3' UTR-MUT) were also amplified and constructed onto the pGL4 vector. Afterwards, the U-CH1 and U-CH2 cells were co-introduced with miR-16-5p or miR-NC and LINC00662-WT, LINC00662-MUT, RNF144B 3' UTR-WT or RNF144B 3' UTR-MUT, respectively. After the transfection for 48 h, the Luciferase activity in U-CH1 and U-CH2 cells was detected using the Dual-Luciferase Reporter Assay Kit (Promega, Madison, WI, USA).

Xenograft Tumor Analysis

BALB/c nude mice (n=12, 6-week-old, male) were purchased from HFK Bioscience Co., LTD (Beijing, China). U-CH1 cells with the transfection of sh-LINC00662 or sh-NC were subcutaneously inoculated into the right flank of mice back. One week after inoculation, the tumor volume was calculated once a week based on the formula: length × width^2 × 0.5. After 5 weeks, all tumor tissues were excised and used for weighting and expression analysis. All animal procedures were approved by the Animal Care and Use Committee of Yantaishan Hospital.

Statistical Analysis

The data were collected from at least three times, independent biological experiments. After the analysis by GraphPad Prism 5.01 (GraphPad Software, Inc., La Jolla, CA, USA), the data were displayed as the mean ± standard deviation (SD). The differences between two groups or among ≥ 3 groups were analyzed by Student's *t*-test or one-way analysis of variance (ANOVA) with Tukey's post-hoc test. The correlation analysis was investigated according to the Spearman's correlation coefficient. $p<0.05$ was considered to be a statistically significant difference.

Results

LINC00662 and RNF144B Were Upregulated in Chordoma Tissues

The expression of LINC00662 and RNF144B was determined in chordoma tissues and adjacent non-tumor tissues. We found that LINC00662 was aberrantly overexpressed in chordoma tissues (n=30) relative to that in non-tumor tissues (n=30) (Figure 1A). Similarly, the expression of RNF144B was also enhanced in chordoma tissues (n=30) relative to that in non-tumor tissues (n=30) at both mRNA and protein levels (Figure 1B and 1C). Besides, Spearman's correlation analysis revealed that the expression of RNF144B at the mRNA levels was positively correlated with LINC00662 expression in chordoma tissues (Figure 1D). The data suggested that the dysregulation of LINC00662 and RNF144B might play crucial roles in chordoma.

LINC00662 Knockdown Inhibited Proliferation, Colony Formation, Migration, Invasion and Epithelial-Mesenchymal Transition (EMT) of Chordoma Cells

The endogenous expression of LINC00662 was knocked down to investigate the role of

LINC00662 in chordoma cells. Firstly, the interference efficiency of LINC00662 was examined, and the result showed that the expression of LINC00662 was significantly reduced in U-CH1 and U-CH2 cells transfected with si-LINC00662 relative to si-NC (Figure 2A). The MTT assay concluded that the proliferation was prominently suppressed in U-CH1 and U-CH2 cells transfected with si-LINC00662 compared with si-NC (Figure 2B and 2C). The number of colonies was also decreased in U-CH1 and U-CH2 cells with the knockdown of LINC00662 (Figure 2D). Besides, the protein levels of cell cycle and proliferation-related markers were ascertained, and the result showed that the levels of Cyclin D1 and Ki67 were pronouncedly declined in U-CH1 and U-CH2 cells transfected with si-LINC00662 compared with si-NC (Figure 2E). Moreover, the transwell assay elucidated that the knockdown of LINC00662 markedly depleted the ability of cell migration and invasion (Figure 2F and 2G). Additionally, the levels of EMT markers were also determined, and the data exhibited that the level of E-cadherin was significantly reinforced, while the levels of Vimentin and N-cadherin were reversely weakened in U-CH1 and U-CH2 cells with the knockdown of LINC00662 (Figure 2H). These data suggested that LINC00662 knockdown blocked the aggression of chordoma cells.

LINC00662 Knockdown Inhibited Glycolysis Progression

The following experiment was conducted to explore the role of LINC00662 in glycolysis progression in chordoma cells. Firstly, the U-CH1 and U-CH2 cells transfected with si-LINC00662 and si-NC were used for the glycolysis stress test. The measurement of ECAR presented that the

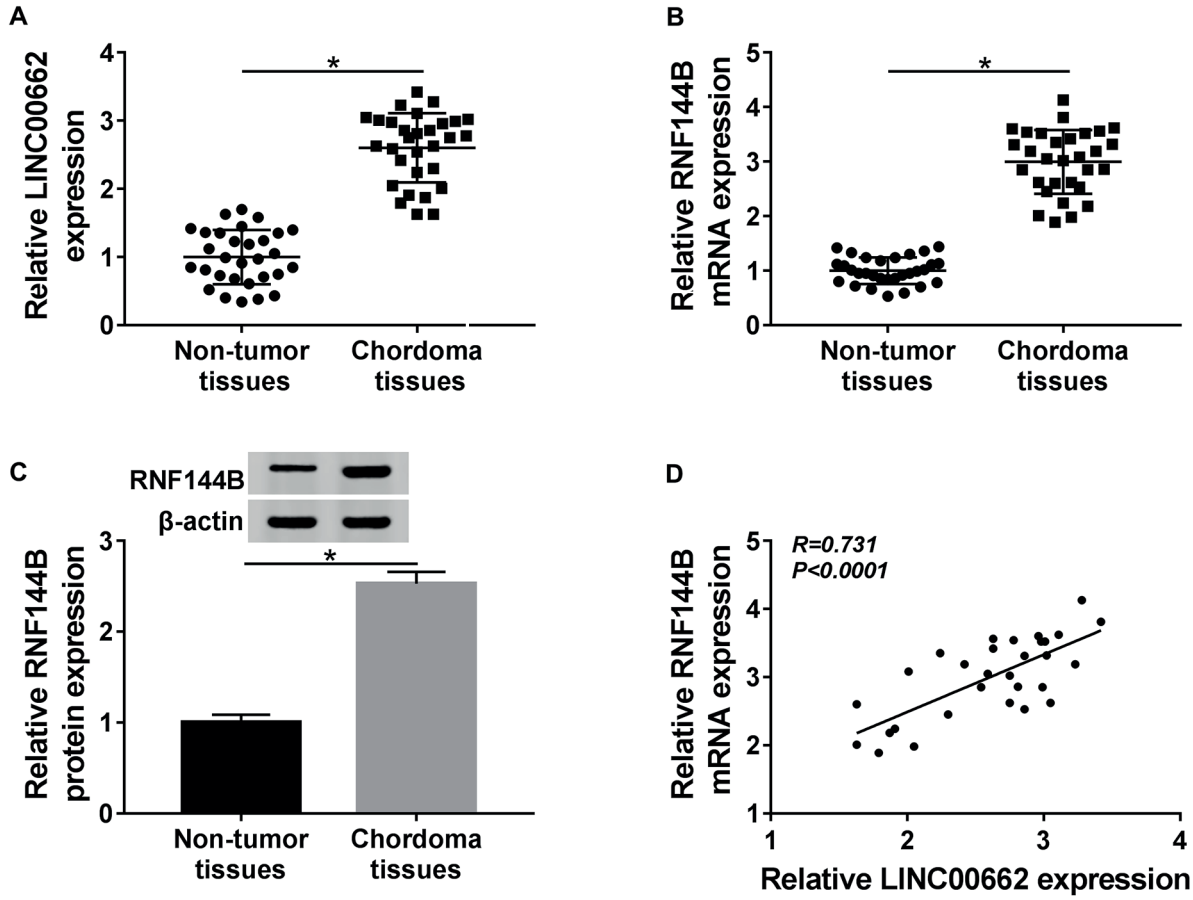

Figure 1. LINC00662 and RNF144B were upregulated in chordoma tissues. **A,** The expression of linc00662 in chordoma tissues and adjacent non-tumor tissues was detected by qRT-PCR. **B,** and **C,** The expression of RNF144B at mRNA and protein levels in chordoma tissues and adjacent non-tumor tissues was detected by qRT-PCR and Western blot. **D,** The expression of RNF144B at mRNA level was negatively correlated with the LINC00662 expression in chordoma tissues. *$p<0.05$.

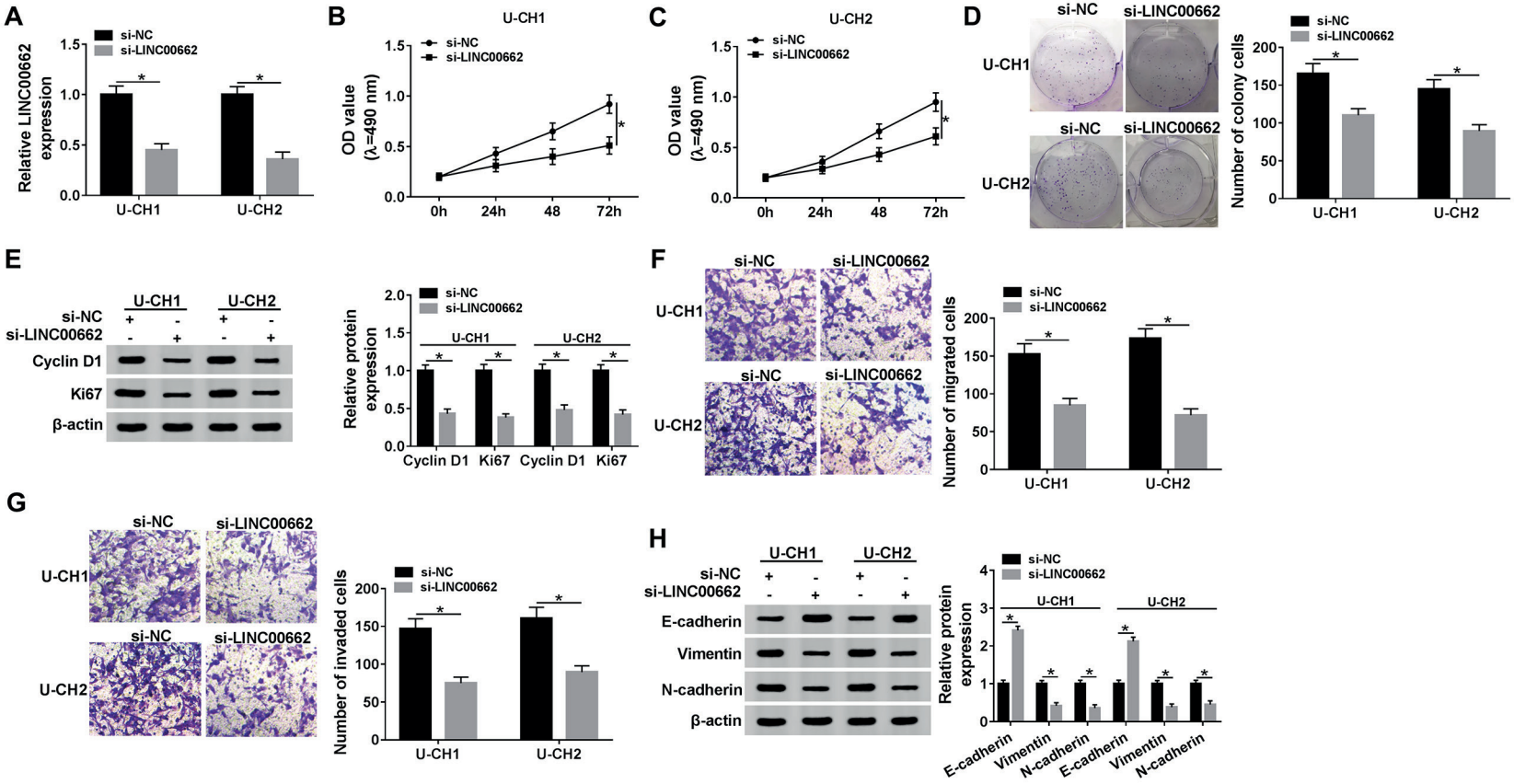

Figure 2. LINC00662 knockdown inhibited proliferation, colony formation, migration, invasion, and EMT of chordoma cells. **A,** The interference efficiency of LINC00662 was measured by qRT-PCR. **B,** and **C,** Cell proliferation was monitored by MTT assay. **D,** The number of colonies was calculated using colony formation assay. **E,** The protein levels of Cyclin D1 and Ki67 were detected by Western blot. **F,** and **G,** Cell migration and invasion were assessed by transwell assay. **H,** The protein levels of E-cadherin, Vimentin and N-cadherin were detected by Western blot. *$p < 0.05$.

addition of glucose increased the level of ECAR, while the level of ECAR in U-CH1 and U-CH2 cells transfected with si-LINC00662 was significantly lower than si-NC, suggesting that high glucose induced glycolysis, and LINC00662 knockdown inhibited the increase of glycolysis relative to si-NC. Then, the oligomycin was added to examine the glycolytic capacity, and we found that the addition of oligomycin strengthened the level of ECAR, while the level of ECAR in U-CH1 and U-CH2 cells transfected with si-LINC00662 was significantly weaker than si-NC, suggesting that LINC00662 knockdown suppressed the glycolytic capacity. Next, the 2-DG was used to block glycolysis, and the result showed that the addition of 2-DG remarkably reduced the level of ECAR, while the level of ECAR in U-CH1 and U-CH2 cells transfected with si-LINC00662 was remarkably lower than si-NC, suggesting that LINC00662 knockdown lessened the glycolytic reserve (Figure 3A-3D). Additionally, we examined the glucose consumption, lactate production, and ATP production, and we noticed that they were all substantially decreased in U-CH1 and U-CH2 cells transfected with si-LINC00662 relative to si-NC (Figure 3E-3G). Moreover, the protein levels of glycolysis-associated indicators were quantified, and we found that the levels of GLUT1, HK2, and LDHA were all weakened in U-CH1 and U-CH2 cells with the knockdown of LINC00662 (Figure 3H). These analyses manifested that the glycolysis progression was enormously impaired after the knockdown of LINC00662.

RNF144B Underrepresentation Blocked Proliferation, Colony Formation, Migration, Invasion, EMT and Glycolysis of Chordoma Cells

To determine the role of RNF144B, U-CH1 and U-CH2 cells were introduced with si-RNF144B or si-NC. Firstly, the interference efficiency test monitored that the expression of RNF144B was conspicuously reduced in si-RNF144B-transfected U-CH1 and U-CH2 cells relative to si-NC at both mRNA and protein levels (Figure 4A and 4B). Cell proliferation was significantly suppressed by RNF144B underrepresentation in U-CH1 and U-CH2 cells (Figure 4C and 4D). The number of colonies was also declined in cells with si-RNF144B transfection compared with si-NC (Figure 4E). Besides, RNF144B underrepresentation dwindled the protein levels of Cyclin D1 and KI67 (Figure 4F). The number of migrated and invaded cells was suppressed in U-CH1 and U-CH2 cells with the knockdown of RNF144B (Figure 4G and 4H). Moreover, the level of E-cadherin was reinforced with the downregulation of RNF144B, while the levels of Vimentin and N-cadherin were depleted (Figure 4I and 4J). In addition, RNF144B underrepresentation strikingly diminished the glycolysis, glycolytic capacity, and glycolytic reserve in U-CH1 and U-CH2 cells as indicated by the measurement of ECAR (Figure 4K-4N). Similarly, RNF144B underrepresentation drastically restrained the glucose consumption, lactate production, and ATP production in U-CH1 and U-CH2 cells (Figure 4O-4Q). Additionally, the protein levels of GLUT1, HK2 and LDHA all plummeted in U-CH1 and U-CH2 cells with si-RNF144B transfection compared with si-NC (Figure 4R). The above data discovered that RNF144B underrepresentation inhibited the aggressive progression of chordoma cells.

RNF144B Overexpression Reversed the Role of LINC00662 Knockdown

U-CH1 and U-CH2 cells were introduced with si-LINC00662 or si-LINC00662+pcDNA-RNF144B, si-NC or si-LINC00662+pcDNA acting as the control, respectively. Firstly, the examination of RNF144B overexpression efficiency showed that the expression of RNF144B was markedly strengthened in U-CH1 and U-CH2 cells transfected with pcDNA-RNF144B relative to pcDNA (Figure 5A and 5B). Then, LINC00662 knockdown-inhibited cell proliferation was recovered in U-CH1 and U-CH2 cells with si-LINC00662+pcDNA-RNF144B transfection but not si-LINC00662+pcDNA (Figure 5C and 5D). Likewise, the number of colonies, inhibited in cells with si-LINC00662 transfection, was restored in cells with si-LINC00662+pcDNA-RNF144B transfection (Figure 5E). The protein levels of Cyclin D1 and Ki67 were weakened by LINC00662 knockdown but regained by the combination of LINC00662 knockdown and RNF144B overexpression (Figure 5F). Besides, the number of migrated and invaded cells was depleted by LINC00662 knockdown but recovered by RNF144B overexpression (Figure 5G and 5H). The protein level of E-cadherin was elevated in U-CH1 and U-CH2 cells transfected with si-LINC00662 but repressed in cells transfected with si-LINC00662+pcDNA-RNF144B, while the levels of Vimentin and N-cadherin were opposite to the level of E-cadherin (Figure 5I). Moreover, LINC00662 knockdown-inhibited glycolysis, glycolytic capacity, and glycolytic reserve were

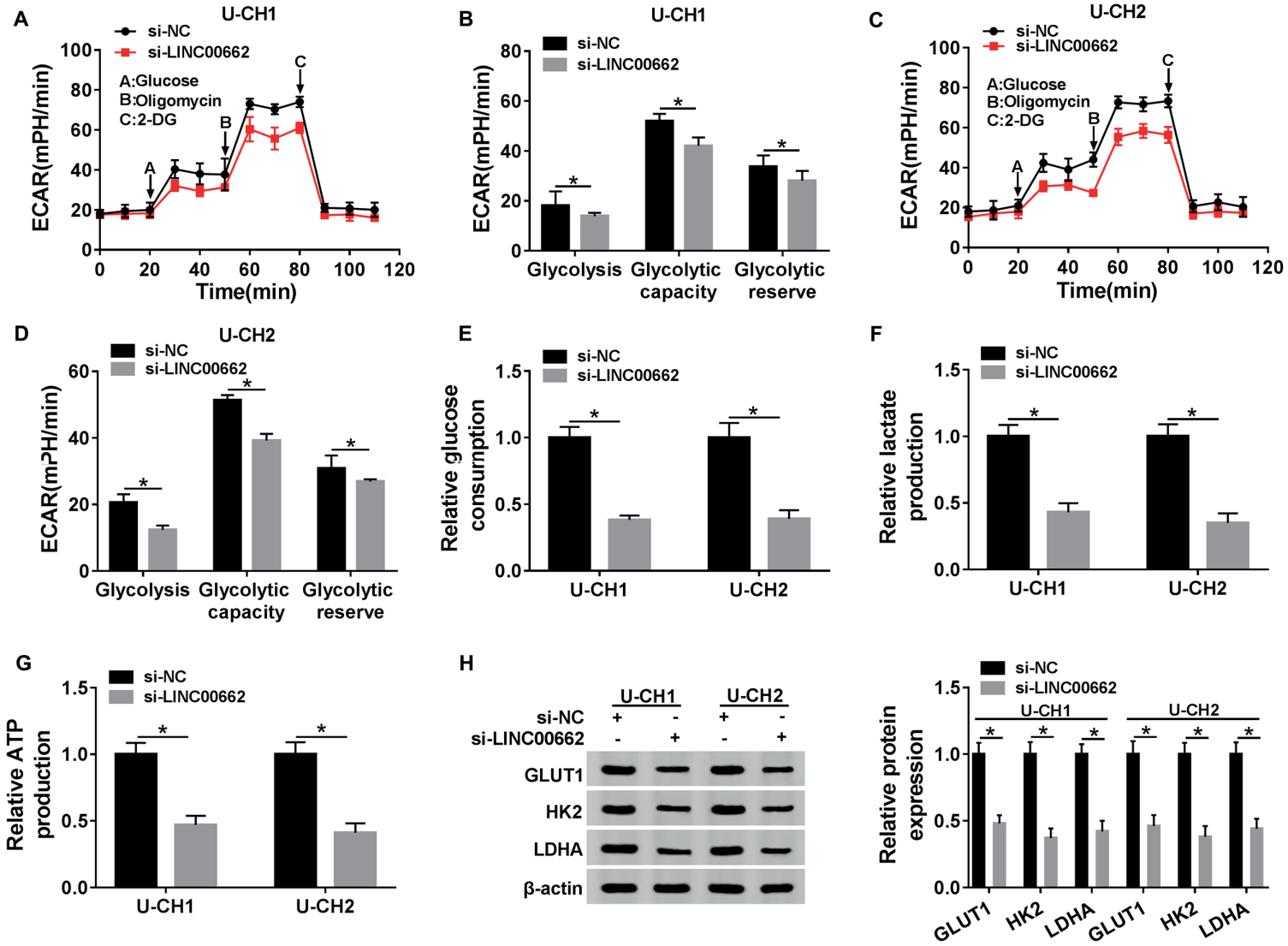

Figure 3. LINC00662 knockdown inhibited glycolysis in chordoma cells. **A,** The detection of ECAR was performed in U-CH1 cells treated with glucose, oligomycin or 2-DG. **B,** The ECAR value was measured to observe glycolysis, glycolytic capacity and glycolytic reserve in U-CH1 cells. **C,** The detection of ECAR was performed in U-CH2 cells treated with glucose, oligomycin or 2-DG. **D,** The ECAR value was measured to observe glycolysis, glycolytic capacity and glycolytic reserve in U-CH2 cells. **E-G,** The glycolysis was assessed by glucose consumption, lactate production, and ATP production. **H,** The protein levels of GLUT1, HK2, and LDHA were quantified by Western blot. *$p < 0.05$.

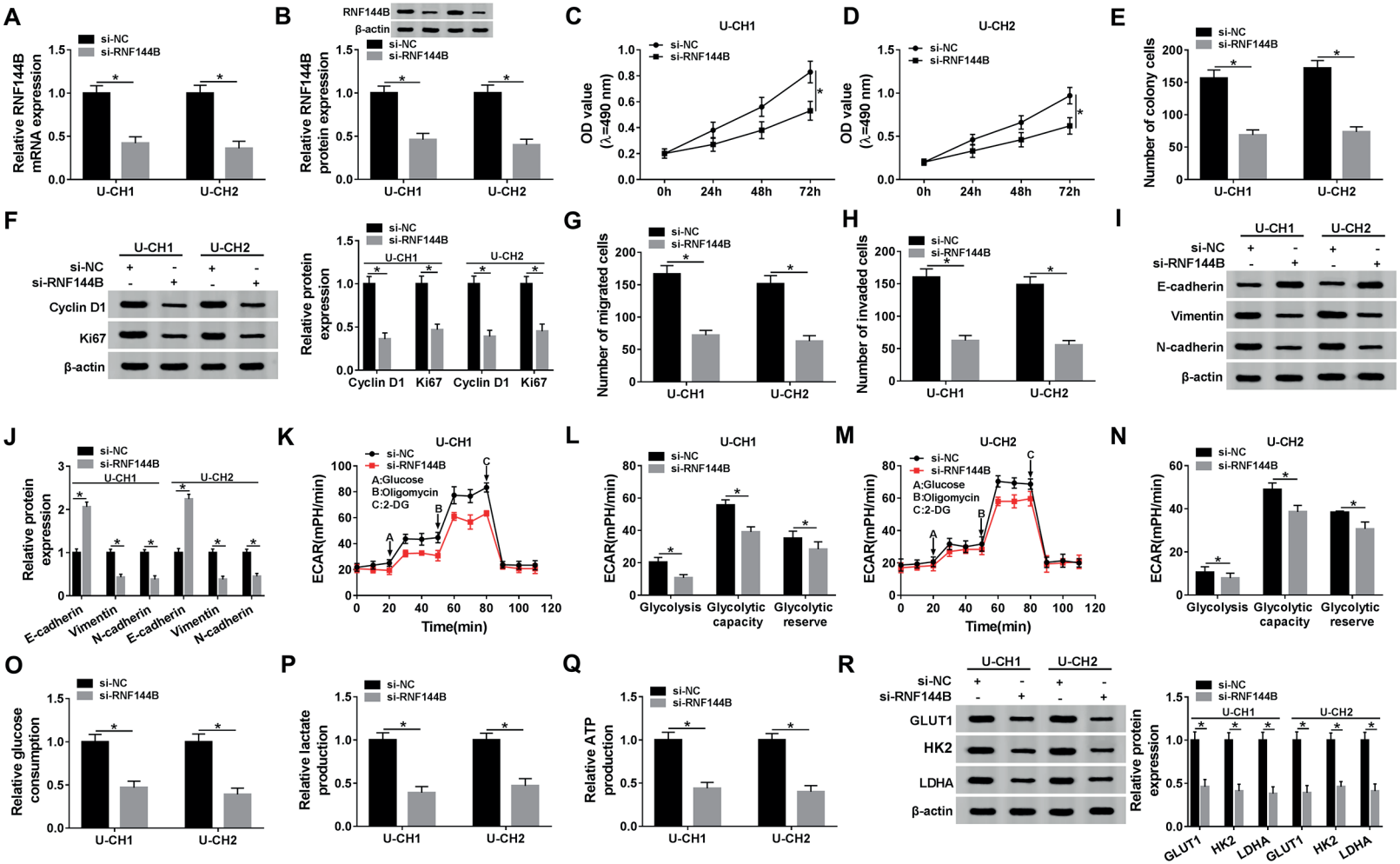

Figure 4. RNF144B knockdown suppressed proliferation, colony formation, migration, invasion, EMT, and glycolysis of chordoma cells. **A,** and **B,** The interference efficiency of RNF144B was measured by qRT-PCR and Western blot. **C,** and **D,** Cell proliferation was monitored by MTT assay. **E,** The number of colonies was calculated using colony formation assay. **F,** The protein levels of Cyclin D1 and Ki67 were detected by Western blot. **G,** and **H,** Cell migration and invasion were assessed by transwell assay. **I,** and **J,** The protein levels of E-cadherin, Vimentin, and N-cadherin were detected by Western blot. **K-N,** The detection of ECAR was performed in U-CH1 and U-CH2 cells treated with glucose, oligomycin or 2-DG to observe glycolysis, glycolytic capacity and glycolytic reserve. **O-Q,** The glycolysis was assessed by glucose consumption, lactate production, and ATP production. **R,** The protein levels of GLUT1, HK2, and LDHA were quantified by Western blot. *$p < 0.05$.

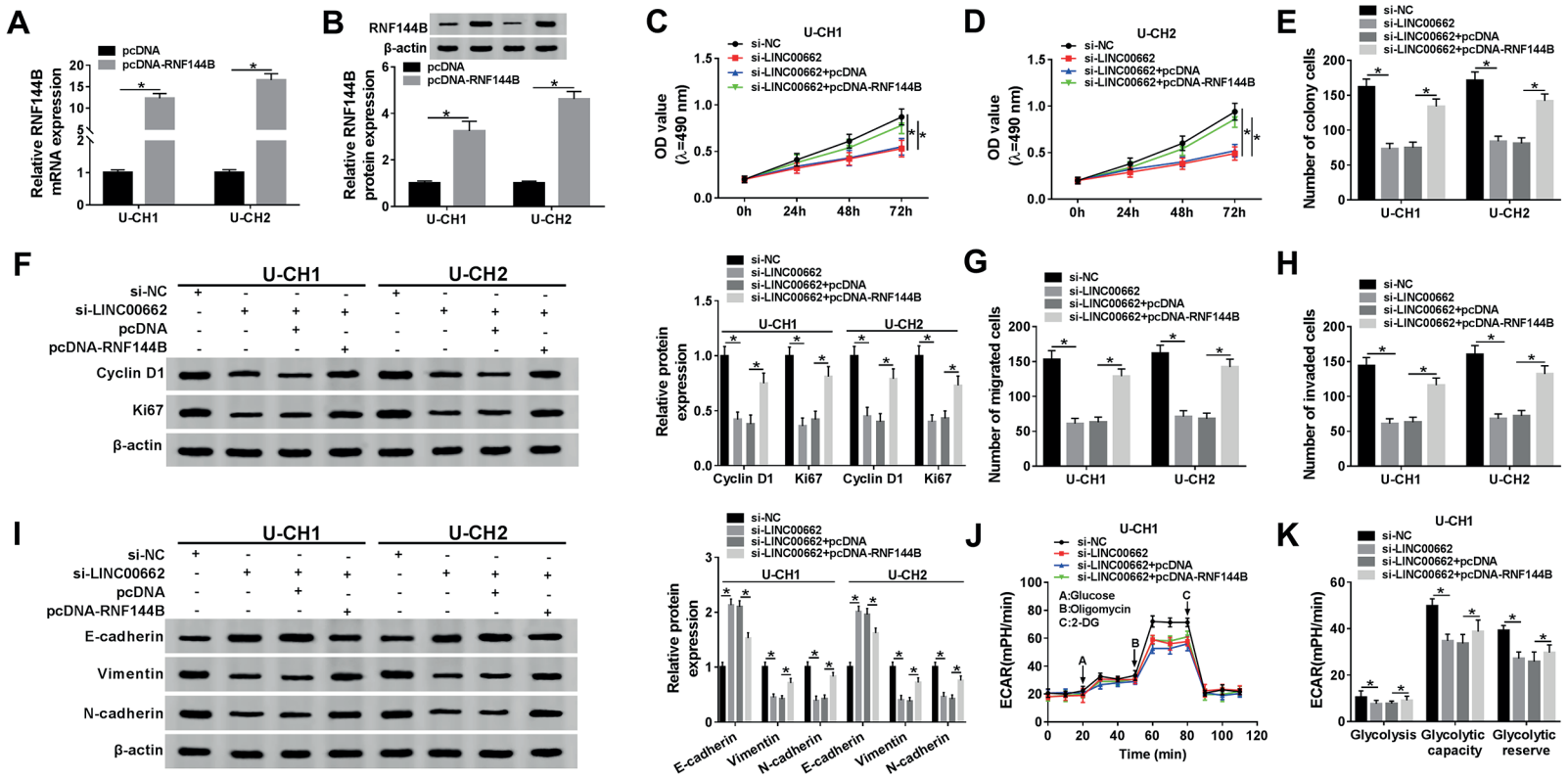

Figure 5. RNF144B overexpression reversed the role of LINC00662 knockdown. **A,** and **B,** The efficiency of RNF144B overexpression was detected by qRT-PCR and Western blot. U-CH1 and U-CH2 cells were transfected with si-LINC00662 or si-LINC00662+pcDNA-RNF144B. **C,** and **D,** Cell proliferation was monitored by MTT assay. **E,** The number of colonies was calculated using colony formation assay. **F,** The protein levels of Cyclin D1 and Ki67 were detected by Western blot. **G,** and **H,** Cell migration and invasion were assessed by transwell assay. **I,** The protein levels of E-cadherin, Vimentin, and N-cadherin were detected by Western blot. **J-M,** The detection of ECAR was performed in U-CH1 and U-CH2 cells treated with glucose, oligomycin or 2-DG to observe glycolysis, glycolytic capacity, and glycolytic reserve.

Figure continued

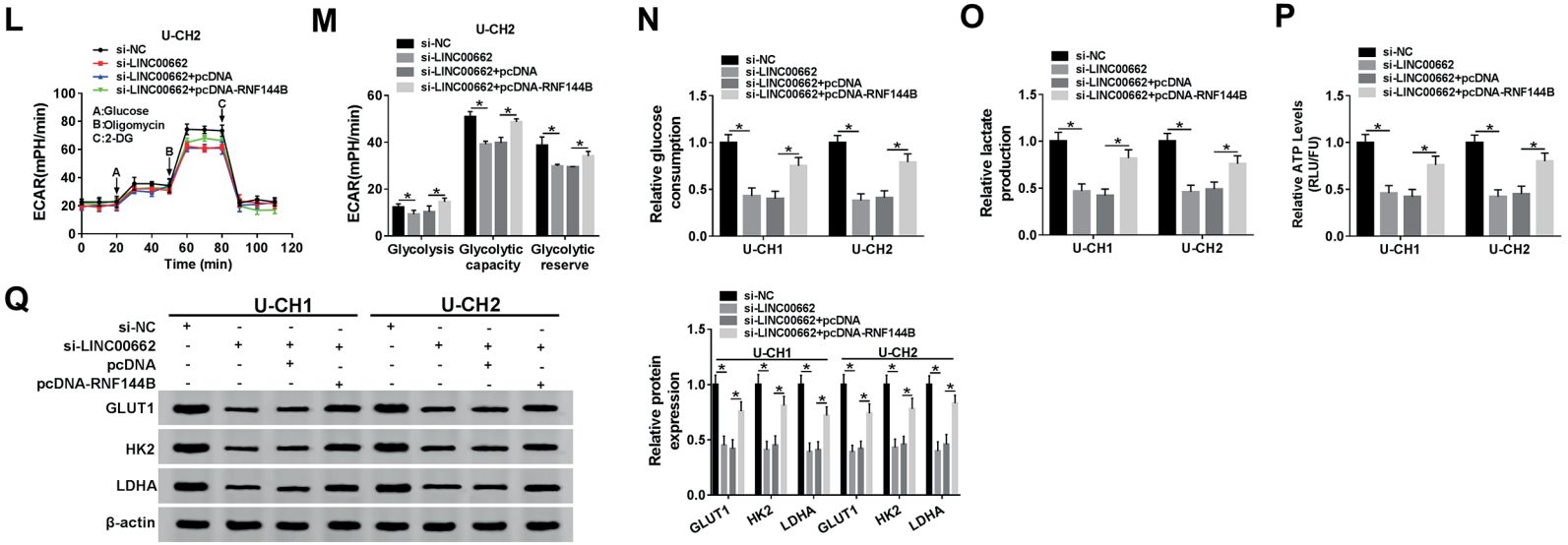

Figure 5. *(Continued).* **J-M,** The detection of ECAR was performed in U-CH1 and U-CH2 cells treated with glucose, oligomycin or 2-DG to observe glycolysis, glycolytic capacity, and glycolytic reserve. **N-P,** The glycolysis was assessed by glucose consumption, lactate production and ATP production. **Q,** The protein levels of GLUT1, HK2 and LDHA were quantified by Western blot. *$p<0.05$.

recovered in U-CH1 and U-CH2 cells transfected with si-LINC00662+pcDNA-RNF144B (Figure 5J-5M). The glucose consumption, lactate production, and ATP production were blocked by LINC00662 knockdown but reestablished by the combination of LINC00662 knockdown and RNF144B overexpression (Figure 5N-5P). Additionally, the protein levels of GLUT1, HK2, and LDHA were suppressed in U-CH1 and U-CH2 cells transfected with si-LINC00662, whereas their levels were restored in cells transfected with si-LINC00662+pcDNA-RNF144B (Figure 5Q). The results clarified that LINC00662 knockdown inhibited the aggressive progression of chordoma cells by decreasing the expression of RNF144B.

MiR-16-5p Acted as a "Bridge" to Connect the Relationship Between LINC00662 and RNF144B

It was well known that lncRNAs contained the miRNA-response elements and could modulate mRNAs by binding to miRNA, thus participating in tumorigenesis and development[24]. Following this manner, we identified the potential target miRNAs of LINC00662. As shown in Figure 6A, miR-16-5p was a target of LINC00662 with special binding sites between them by the prediction of starBase (http://starbase.sysu.edu.cn/). Also, RNF144B was a target of miR-16-5p with specific binding sites between RNF144B 3'UTR and miR-16-5p (Figure 6A). Next, Dual-Luciferase reporter assay was performed to confirm this prediction, and the result indicated that the miR-16-5p reintroduction significantly weakened the Luciferase activity in U-CH1 and U-CH2 cells transfected with LINC00662-WT but nor LINC00662 MUT compared with miR-NC (Figure 6B and 6C). Besides, the miR-16-5p reintroduction also notably reduced the Luciferase activity in U-CH1 and U-CH2 cells with RNF144B 3' UTR-WT but not RNF144B 3' UTR-MUT relative to miR-NC (Figure 6D and 6E). Moreover, we found that the expression of miR-16-5p in U-CH1 and U-CH2 cells transfected with si-LINC00662 was declined relative to si-NC (Figure 6F). Afterwards, the endogenous level of miR-16-5p was weakened to observe the effects of miR-16-5p on the expression of RNF144B. The inhibition efficiency of miR-16-5p showed that the expression of miR-16-5p was markedly declined in U-CH1 and U-CH2 cells transfected with anti-miR-16-5p relative to anti-NC (Figure 6G). Not surprisingly, the expression of RNF144B was considerably increased with the inhibition of miR-16-5p at both mRNA and protein levels (Figure 6H and 6I). Additionally, the expression of RNF144B was decreased in U-CH1 and U-CH2 cells transfected with si-LINC00662 but recovered in cells transfected with si-LINC00662+anti-miR-16-5p at both mRNA and protein levels (Figure 6J and 6K). These data proved that LINC00662 regulated the expression of RNF144B by targeting miR-16-5p.

LINC00662 Knockdown Inhibited Tumor Growth In Vivo

U-CH1 cells were transfected with sh-LINC00662 to investigate the role of LINC00662 *in vivo*, sh-NC acting as the control. The tumor volume was recorded once a week, and the data showed that the tumor volume was significantly declined with the knockdown of LINC00662 (Figure 7A). Besides, LINC00662 also dwindled the tumor weight compared with sh-NC (Figure 7B). Additionally, the expression of LINC00662 in excised tissues from the sh-LINC00662 group was notably reduced compared with that in the sh-NC group, while the expression of miR-16-5p was opposite to LINC00662 expression (Figure 7C and 7D). The expression of RNF144B was notably decreased in excised tissues from the sh-LINC00662 group was, which was notably reduced relative to that in the sh-NC group at both mRNA and protein levels (Figure 7E and 7F). The data indicated that LINC00662 knockdown inhibited the tumor growth *in vivo* through the regulation of miR-16-5p and RNF144B.

Discussion

Chordoma is a rare malignancy tumor with a low incidence of 0.08 per 100,000[25]. Unfortunately, the development of chordoma is associated with severe local aggressiveness, and massive masses to damage nerves and blood vessels[26]. Besides, chordoma is insensitive to the radiotherapy and drug chemotherapy, and surgery seems to be a leading therapeutic strategy. However, the complexity of the spinal anatomy and considerable tumor size present significant challenges for surgery[25,27]. Therefore, it is urgent to find novel therapeutic strategies to improve treatment effects.

In view of the imperative role of lncRNAs in cancers, lncRNAs are promising candidates for the diagnosis and therapy of cancers[28]. Our data showed the carcinogenic effects of LINC00662 on chordoma. The similar role of LINC00662 was demonstrated in numerous cancers. For ex-

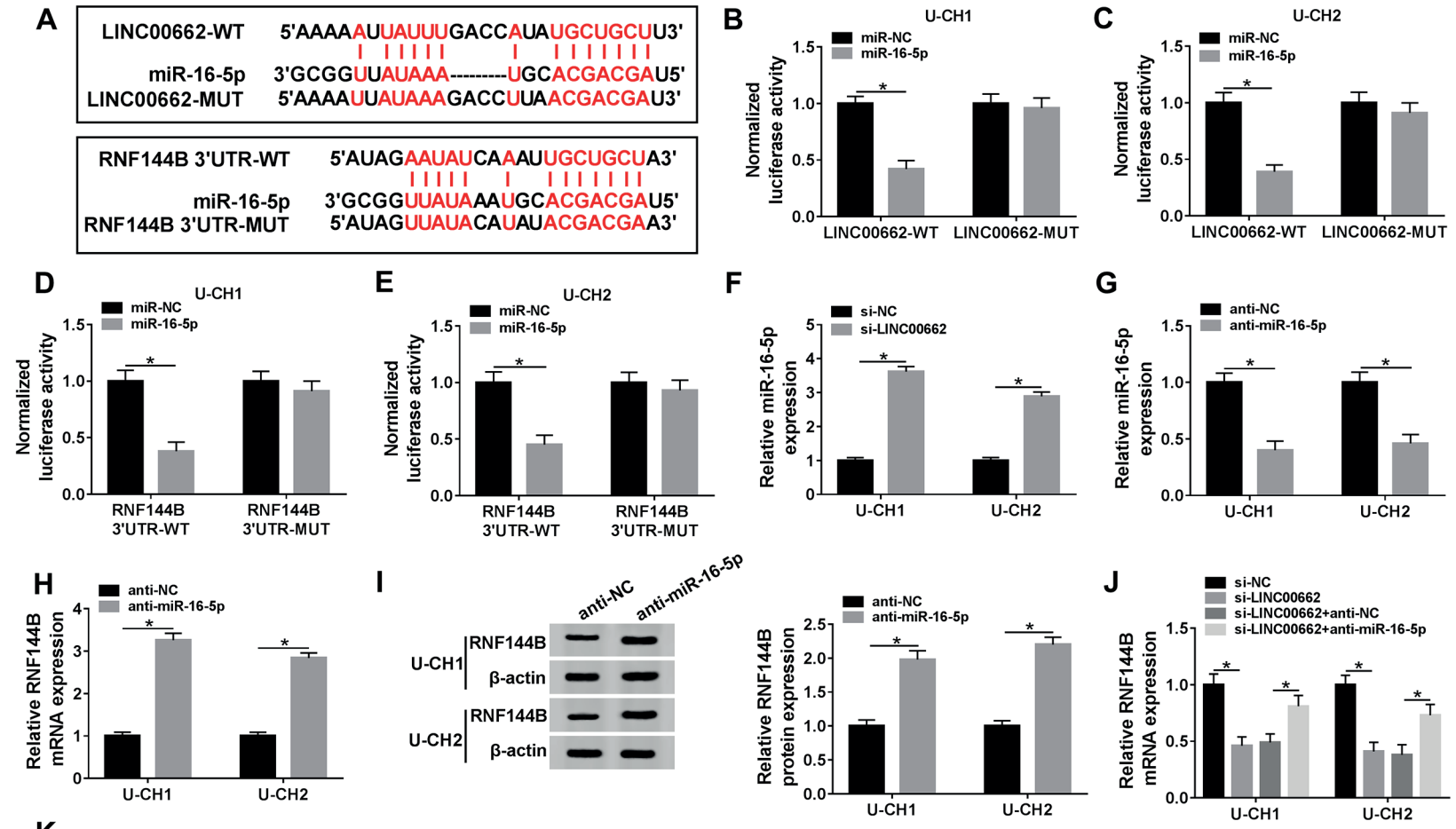

Figure 6. LINC00662 bound to miR-16-5p, and RNF144B was a target of miR-16-5p. **A,** The relationship between miR-16-5p and LINC00662 or RNF144B was predicted by the online tool starBase. **B,** and **C,** The relationship between miR-16-5p and LINC00662 was verified by Dual-Luciferase reporter assay. **D,** and **E,** The relationship between miR-16-5p and RNF144B was verified by Dual-Luciferase reporter assay. **F,** The effect of LINC00662 knockdown on miR-16-5p expression was assessed by qRT-PCR. **G,** The efficiency of miR-16-5p inhibition was evaluated by qRT-PCR. **H,** and **I,** The effect of miR-16-5p inhibition on RNF144B expression at both mRNA and protein levels was assessed by qRT-PCR and Western blot. **J,** and **K,** The expression of RNF144B at both mRNA and protein levels was determined in U-CH1 and U-CH2 cells transfected with si-LINC00662, si-NC, si-LINC00662+anti-miR-16-5p or si-LINC00662+anti-NC. *$p < 0.05$.

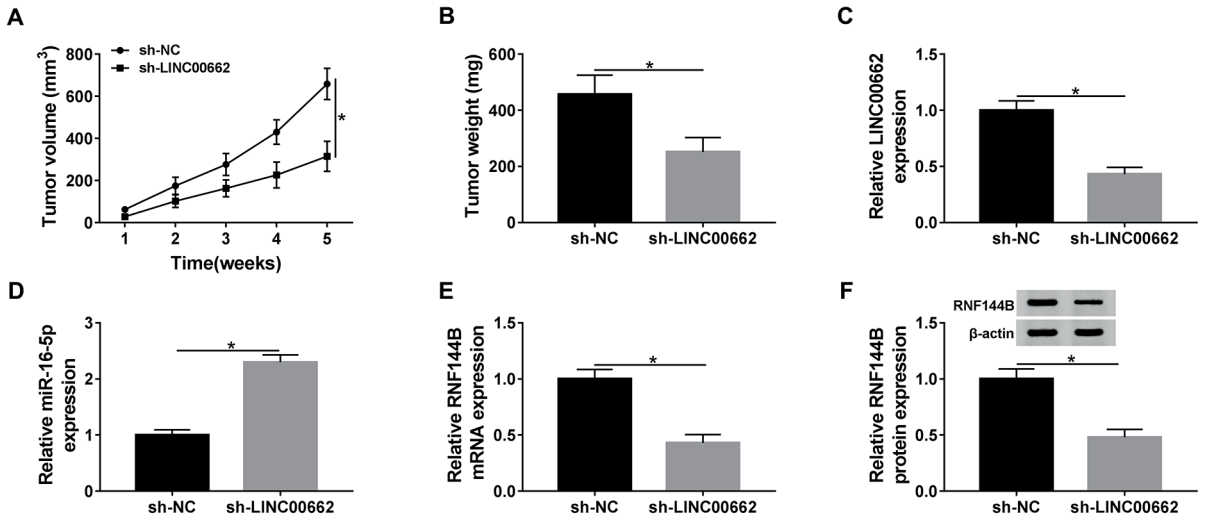

Figure 7. LINC00662 knockdown inhibited tumor growth *in vivo*. U-CH1 cells transfected with sh-LINC00662 or sh-NC were injected into the nude mice. **A,** The tumor volume was recorded once a week. **B,** The tumor weight was measured after five weeks when the mice were killed. **C,** and **D,** The expression of LINC00662 and miR-16-5p was detected in excised tumor tissues by qRT-PCR. **E,** and **F,** The expression of RNF144B at mRNA and protein levels was detected by qRT-PCR and Western blot. *$p<0.05$.

ample, LINC00662 overexpression was linked to the undesirability prognosis of patients with lung cancer, and upregulation of LINC00662 promoted cell migration and invasion *in vitro*[29]. Likewise, LINC00662 was observed to be upregulated in gastric cancer tissues and cells, and its knockdown reduced proliferation and chemoresistance of gastric cancer cells[30]. In agreement with the role of LINC00662 in other cancers, our study, for the first time concluded that LINC00662 was aberrantly expressed with a high level in chordoma tissues. Furthermore, its interference blocked the progression of chordoma cells through the inhibition of proliferation, colony formation, migration, invasion, and glycolysis *in vitro* and inhibited tumor growth *in vivo*, suggesting that LINC00662 was an oncogene in chordoma. Recently, the research of metabolism emerges in the development of numerous human diseases because glucose metabolism is the main mean of energy acquisition in living organisms[31]. The link between aerobic glycolysis and tumorigenesis has been previously described as the "Warburg effect"[32]. As a consequence, the dysregulation of metabolism is identified as one of the most important indicators of cancer progression[33]. Wang et al[34] declared that fulvestrant inhibited prolactinoma by blocking cellular glycolysis through a special signaling pathway. Interestingly, LINC00662 was also involved in the regulation of glycolysis, which enriched the functional role of LINC00662.

It has been elaborated that lncRNAs serve as competing endogenous RNA (ceRNA) to adsorb miRNAs and mediate their biological function[24]. Following this regulatory manner, the underlying target miRNAs of LINC00662 were identified, and miR-16-5p was forecasted and verified as one of the targets of LINC00662. The document about LINC00662 or miR-16-5p in accordance with this regulatory mode was mentioned in previous studies. So, LINC00662 accelerated the malignant development of acute myeloid leukemia cells by modulating ROCK1 by targeting miR-340-5p[35]. LncRNA PVT1 contributed to proliferation, invasion, and EMT by sponging miR-16-5p and inhibiting its expression[23]. The tumor suppressor role of miR-16-5p was also introduced in other cancers, such as hepatocellular carcinoma[36]. Additionally, we verified that miR-16-5p bound to the 3' UTR of RNF144B and modulated the expression of RNF144B.

RNF144B was reported to be a potential biomarker to promote cell proliferation by activating the GSK3β activity in endometrial cancer[22]. Besides, miR-100 inhibition interdicted ubiquitin-mediated p53 protein degradation *via* inducing RNF144B, leading to the mediation of cell apop-

tosis in gastric cancer[37]. These data introduced us to realize the important role of RNF144B in cancers. Interestingly, the role of RNF144B was investigated in a previous study, and the result presented that RNF144B downregulation restrained cell proliferation, migration, and invasion but advanced cell apoptosis in chordoma cells[11]. Consistent with the result from this research, our data proved that RNF144B was highly expressed in chordoma tissues, and its knockdown blocked proliferation, colony formation, migration, invasion, EMT, and glycolysis. These consequences maintained that RNF144B was an oncogene at least in chordoma. Further exploration manifested that RNF144B overexpression rescued the effects of LINC00662 knockdown, and the interaction between LINC00662 and RNF144B was linked by miR-16-5p.

Conclusions

Summarily, the expression of LINC00662 and RNF144B was aberrantly elevated in chordoma tissues. Functional experiments alleged that the knockdown of LINC00662 or RNF144B suppressed chordoma progression *in vitro* by the block of cell proliferation, colony formation, migration, invasion, EMT, and glycolysis. Mechanism analysis revealed that LINC00662 exerted its role by activating RNF144B *via* sponging miR-16-5p. Our study supplied a theoretical basis for the mechanism of chordoma development and provided novel biomarkers for the diagnosis and treatment of chordoma.

Conflict of Interests

The Authors declare that they have no conflict of interests.

References

1) Smoll NR, Gautschi OP, Radovanovic I, Schaller K, Weber DC. Incidence and relative survival of chordomas: the standardized mortality ratio and the impact of chordomas on a population. Cancer 2013; 119: 2029-2037.
2) McMaster ML, Goldstein AM, Bromley CM, Ishibe N, Parry DM. Chordoma: incidence and survival patterns in the United States, 1973-1995. Cancer Causes Control 2001; 12: 1-11.
3) Ma Y, Zhu B, Liu X, Liu Z, Jiang L, Wei F, Yu M, Wu F, Zhou H, Xu N, Liu X, Yong L, Wang Y, Wang P, Liang C, He G. iASPP overexpression is associated with clinical outcome in spinal chordoma and influences cellular proliferation, invasion, and sensitivity to cisplatin in vitro. Oncotarget 2017; 8: 68365-68380.
4) Chugh R, Tawbi H, Lucas DR, Biermann JS, Schuetze SM, Baker LH. Chordoma: the nonsarcoma primary bone tumor. Oncologist 2007; 12: 1344-1350.
5) Rinner B, Weinhaeusel A, Lohberger B, Froehlich EV, Pulverer W, Fischer C, Meditz K, Scheipl S, Trajanoski S, Guelly C, Leithner A, Liegl B. Chordoma characterization of significant changes of the DNA methylation pattern. PLoS One 2013; 8: e56609.
6) Kishimoto R, Omatsu T, Hasegawa A, Imai R, Kandatsu S, Kamada T. Imaging characteristics of metastatic chordoma. Jpn J Radiol 2012; 30: 509-516.
7) Heery CR. Chordoma: the quest for better treatment options. Oncol Ther 2016; 4: 35-51.
8) Quinn JJ, Chang HY. Unique features of long non-coding RNA biogenesis and function. Nat Rev Genet 2016; 17: 47-62.
9) Flynn RA, Chang HY. Long noncoding RNAs in cell-fate programming and reprogramming. Cell Stem Cell 2014; 14: 752-761.
10) Schmitt AM, Chang HY. Long noncoding RNAs in cancer pathways. Cancer Cell 2016; 29: 452-463.
11) Ma X, Qi S, Duan Z, Liao H, Yang B, Wang W, Tan J, Li Q, Xia X. Long non-coding RNA LOC554202 modulates chordoma cell proliferation and invasion by recruiting EZH2 and regulating miR-31 expression. Cell Prolif 2017; 50. doi: 10.1111/cpr.12388. Epub 2017 Sep 30.
12) Ransohoff JD, Wei Y, Khavari PA. The functions and unique features of long intergenic non-coding RNA. Nat Rev Mol Cell Biol 2018; 19: 143-157.
13) Chan JJ, Tay Y. Noncoding RNA: RNA regulatory networks in cancer. Int J Mol Sci 2018; 19. pii: E1310. doi: 10.3390/ijms19051310.
14) Gebert LFR, MacRae IJ. Regulation of microRNA function in animals. Nat Rev Mol Cell Biol 2019; 20: 21-37.
15) Ambros V. The functions of animal microRNAs. Nature 2004; 431: 350-355.
16) Lou W, Liu J, Gao Y, Zhong G, Chen D, Shen J, Bao C, Xu L, Pan J, Cheng J, Ding B, Fan W. MicroRNAs in cancer metastasis and angiogenesis. Oncotarget 2017; 8: 115787-115802.
17) Ruan L, Qian X. MiR-16-5p inhibits breast cancer by reducing AKT3 to restrain NF-kappaB pathway. Biosci Rep 2019; 39. pii: BSR20191611. doi: 10.1042/BSR20191611.
18) Liu GP, Wang WW, Lu WY, Shang AQ. The mechanism of miR-16-5p protection on LPS-induced A549 cell injury by targeting CXCR3. Artif Cells Nanomed Biotechnol 2019; 47: 1200-1206.
19) Munson PB, Hall EM, Farina NH, Pass HI, Shukla A. Exosomal miR-16-5p as a target for malignant mesothelioma. Sci Rep 2019; 9: 11688.
20) Zhang H, Yang K, Ren T, Huang Y, Tang X, Guo W. miR-16-5p inhibits chordoma cell proliferation, in-

vasion and metastasis by targeting Smad3. Cell Death Dis 2018; 9: 680.

21) Conforti F, Yang AL, Piro MC, Mellone M, Terrinoni A, Candi E, Tucci P, Thomas GJ, Knight RA, Melino G, Sayan BS. PIR2/Rnf144B regulates epithelial homeostasis by mediating degradation of p21WAF1 and p63. Oncogene 2013; 32: 4758-4765.

22) Zhou Q, Eldakhakhny S, Conforti F, Crosbie EJ, Melino G, Sayan BS. Pir2/Rnf144b is a potential endometrial cancer biomarker that promotes cell proliferation. Cell Death Dis 2018; 9: 504.

23) Ren Y, Huang W, Weng G, Cui P, Liang H, Li Y. LncRNA PVT1 promotes proliferation, invasion and epithelial-mesenchymal transition of renal cell carcinoma cells through downregulation of miR-16-5p. Onco Targets Ther 2019; 12: 2563-2575.

24) Zhang Y, Xu Y, Feng L, Li F, Sun Z, Wu T, Shi X, Li J, Li X. Comprehensive characterization of lncRNA-mRNA related ceRNA network across 12 major cancers. Oncotarget 2016; 7: 64148-64167.

25) Walcott BP, Nahed BV, Mohyeldin A, Coumans JV, Kahle KT, Ferreira MJ. Chordoma: current concepts, management, and future directions. Lancet Oncol 2012; 13: e69-76.

26) Casali PG, Stacchiotti S, Sangalli C, Olmi P, Gronchi A. Chordoma. Curr Opin Oncol 2007; 19: 367-370.

27) Stacchiotti S, Casali PG, Lo Vullo S, Mariani L, Palassini E, Mercuri M, Alberghini M, Pilotti S, Zanella L, Gronchi A, Picci P. Chordoma of the mobile spine and sacrum: a retrospective analysis of a series of patients surgically treated at two referral centers. Ann Surg Oncol 2010; 17: 211-219.

28) Shi T, Gao G, Cao Y. Long noncoding RNAs as novel biomarkers have a promising future in cancer diagnostics. Dis Markers 2016; 2016: 9085195.

29) Gong W, Su Y, Liu Y, Sun P, Wang X. Long non-coding RNA Linc00662 promotes cell invasion and contributes to cancer stem cell-like phenotypes in lung cancer cells. J Biochem 2018; 164: 461-469.

30) Liu Z, Yao Y, Huang S, Li L, Jiang B, Guo H, Lei W, Xiong J, Deng J. LINC00662 promotes gastric cancer cell growth by modulating the Hippo-YAP1 pathway. Biochem Biophys Res Commun 2018; 505: 843-849.

31) Li M, Jia F, Zhou H, Di J, Yang M. Elevated aerobic glycolysis in renal tubular epithelial cells influences the proliferation and differentiation of podocytes and promotes renal interstitial fibrosis. Eur Rev Med Pharmacol Sci 2018; 22: 5082-5090.

32) Warburg O. On the origin of cancer cells. Science 1956; 123: 309-314.

33) Hanahan D, Weinberg RA. Hallmarks of cancer: the next generation. Cell 2011; 144: 646-674.

34) Wang C, Xu JL, Wen Y, Zhang DZ, Wang X, Chang L, Li GF, Xie LY, Su J, Zhang XX, Tan CL. Fulvestrant inhibits the glycolysis of prolactinoma GH3 cells by downregulating IRE1/XBP1 signaling pathway. Eur Rev Med Pharmacol Sci 2018; 22: 5364-5370.

35) Cheng B, Ding F, Huang CY, Xiao H, Fei FY, Li J. Role of miR-16-5p in the proliferation and metastasis of hepatocellular carcinoma. Eur Rev Med Pharmacol Sci 2019; 23: 137-145.

36) Liu Y, Gao X, Tian X. High expression of long intergenic non-coding RNA LINC00662 contributes to malignant growth of acute myeloid leukemia cells by upregulating ROCK1 via sponging microRNA-340-5p. Eur J Pharmacol 2019; 859: 172535.

37) Yang G, Gong Y, Wang Q, Wang L, Zhang X. miR-100 antagonism triggers apoptosis by inhibiting ubiquitination-mediated p53 degradation. Oncogene 2017; 36: 1023-1037.